Macromolecular Research, Vol. 11, No. 4, pp 241-249 (2003)

Phase Behaviors of Binary Protein Systems: Consideration of Structural Effects

Sang Gon Kim, Sung Ho Kong, and Young Chan Bae*

Division of Chemical Engineering, Hanyang University, Seoul 133-791, Korea

Sunjoon Kim

Department of Environmental Geosystem Engineering, Hanyang University, Seoul 133-791, Korea

Received Dec. 7, 2002; Revised June 3, 2003

Abstract: A molecular-thermodynamic model to describe the salt-induced protein precipitation is developed based on the perturbation theory. We employed the modified perturbed hard-sphere-chain (PHSC) equation of state for copolymer mixtures to take into account the pre-aggregation effect among protein particles. Hypothetical pressure-composition diagrams are computed with various size differences and salt concentrations. The precipitation behaviors are also studied for various types of pre-aggregation effect for the given systems.

Keywords: pre-aggregation, binary protein system, interaction potentials, phase equilibria.

Introduction

In early days of protein chemistry, the only practical way of separating different types of protein was by causing part of a mixture to precipitate through the alternation of some property of the solvent. Protein precipitation is the simplest and the oldest practical way to separate different proteins from a solution mixture. Separation is achieved through the addition of precipitation agents such as inorganic salts, non-ionic polymers, polyelectrolytes, and organic solvents.[1-5] Salt-induced precipitation has been successfully applied for separating proteins in downstream processing.[6,7] For the efficient design of a protein separation process, a good understanding of the phase behavior of proteins in aqueous electrolyte solutions is helpful.

A variety of researches for the protein precipitation behavior have been studied by using various experimental techniques. Coen *et al.*[8] studied the salting-out phase equilibria for lysozyme and α-chymotrypsin from the concentrated ammonium-sulfate solution. Shih *et al.*[3] observed the solubility of lysozyme, α-chymotrypsin and bovine serum albumin in an aqueous electrolyte solution as a function of ionic strength, pH, the chemical nature of salt, and the initial protein concentration. Wu *et al.*[9] measured the osmotic pressures of the bovine serum albumin aqueous solution at various salt concentration and solution pH. Theoretically, many researchers[10-17] (Verwey and Overbeek, 1948; Asakura and Oosawa, 1958; Vrij, 1976; Joanny *et al.*, 1979; De Hek and Vrij, 1995; Gast *et al.*, 1983b; Grimson, 1983; Victor and Hansen, 1984) reported models to describe the phase behaviors of these complex systems by using the one-component mean-force potential approximation. Mahadevan and Hall,[18,19] Vlachy and Prausnitz[20,21] have used the model to describe aqueous globular proteins in solutions of low salt concentration, and Chiew *et al.*[22] and Kuehner *et al.*[23] used a similar approach for solutions of high salt concentartion. A reliable molecular thermodynamic model for the satisfactory description of the phase behavior of a protein solution relies on an accurate potential of mean force between protein molecules at various solution conditions. Thermodynamic properties and phase-separation conditions of protein solutions described by such models have been computed using a number of different satistical-mechanical approximation methods. These methods can be charaterized based on the osmotic virial expansion, statistical-mechanical perturbation theory, integral-equation theory, and the random-phase approximation.

In our previous work,[24] we proposed an equation of state for a single protein system based on Chiew's model for homopolymers to take into account the pre-aggregation effect[24,35] among protein particles.

In binary protein systems, the pre-aggregation is expected to occur between different protein particles as well as single ones. A simple chain-connectivity which is employed to the pre-aggregation for single protein system, therefore, cannot be mixtures composed of different proteins. Song *et al.*[25-27] and Hino *et al.*[28,29] recently proposed a perturbed hard-sphere-

*e-mail : ycbae@hanyang.ac.kr

chain (PHSC) equation of state for copolymer mixtures based on a modified form of Chiew's equation of state for athermal mixtures of heteronuclear hard-sphere chains. On the assumption that the pre-aggregated protein mixture has a structural similarity to copolymers, the PHSC equation of state can be employed to describe those behaviors of protein mixtures.

In this study, we propose a molecular thermodynamic model for the binary protein systems to explain the effect of pre-aggregations among protein particles. We investigate the effect of size disparities and salt concentrations on the osmotic pressure. The influence of protein pre-aggregation for different types of proteins is also discussed.

Theoretical Consideration

Protein-Protein Potentials. The overall perturbation potential of mean force between two different protein molecules, $W_{ij}^{overall}$, is given by the sum of four potentials of mean force

$$W_{ij}^{overall}(r) = W_{ij}^{elec}(r) + W_{ij}^{disp}(r) + W_{ij}^{osmotic}(r) + W_{ij}^{specific}(r) \quad (1)$$

where r is the center to center separation length. W_{ij}^{elec} is the electric double-layer-repulsion potential, $W_{ij}^{disp}(r)$ is the dispersion potential of Hamaker, $W_{ij}^{osmotic}(r)$ is an attractive interaction due to the excluded-volume effect of the salt ions, and $W_{ij}^{specific}$ is an attractive potential between proteins due to any specific chemical effects such as hydrophobic interactions. Appendix 2 provides expressions for the various potentials of mean force.

Equation of State. In perturbation theory, an assembly of hard spheres is used as the reference system, while the remaining interactions are treated as perturbations;

$$\frac{P}{\rho kT} = \left(\frac{P}{\rho kT}\right)_{ref} + \left(\frac{P}{\rho kT}\right)_{pert} \quad (2)$$

where ρ is the density of protein molecules, and P is the pressure.

Binary Protein System. Derivation of the equation of state for mixtures follows a rigorous first-order statistical-mechanical perturbation theory based on the mixture of hard-spheres as a reference system.

Fluid Phase. The equation of state for fluid mixtures is given

$$\left(\frac{P}{kT}\right)_{fluid} = \left(\frac{P}{kT}\right)_{fluid,ref} + \left(\frac{P}{kT}\right)_{fluid,pert} \quad (3)$$

We assume that protein particles exist as an aggregated form due to the presence of the hydrophobic group on the protein surface before the separation process. It strongly influences on the separation behavior and is defined as a pre-aggregation.

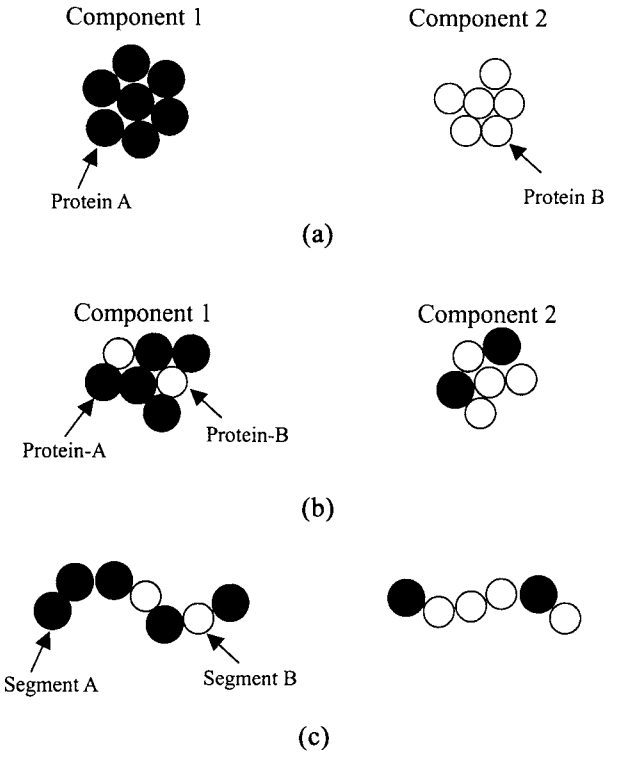

Figure 1. Schematic of homo-type pre-aggregated components (a), hetero-type pre-aggregated components consisting of protein-A and B (b) and two types of random copolymer consisting of segments A and B (c).

For a binary protein system, a pre-aggregation is expected to occur between not only homogeneous proteins (see Figure 1(a)) but also heterogeneous ones (see Figure 1(b)) owing to the properties of various types of protein molecules.

The structure of the pre-aggregated binary protein particles is assumed to be the same as that of the folded random copolymer that is composed of segments A and B (see Figure 1(b) and (c)). In a binary protein system, segments A and B represent protein-A and protein-B, respectively, and the chain length dependent parameter for the copolymer can be directly used as a degree of pre-aggregation. In this work, we consider the pre-aggregated proteins as the type of $(A_XB_{1-X})_{\omega_1}/(A_YB_{1-Y})_{\omega_2}$, where X and Y are fractions of the protein-A in the component-1 and component-2, respectively, ω_1 and ω_2 are the degree of pre-aggregation in each component.

In this system, the formation of the pre-aggregation is altered with values of fractions of proteins in each component, X and Y; $X = 1$ and $Y = 0$ means homo-type pre-aggregation (Figure 1(a)), and $X<1$ and $Y>0$ means a hetero-type pre-aggregation (Figure 1(b)).

The pre-aggregation is assumed to occur in homogeneous protein particles more easily than those of heterogeneous

ones (i.e., X>0.5 and Y<0.5). Component-1 and component-2 mean protein-A rich and protein-B rich components, respectively.

The reference equation for the copolymer mixtures is given

$$\left(\frac{P}{\rho kT}\right)_{ref} = 1+\rho\sum_{i=1}^{m}\sum_{j=1}^{m}x_i x_j\left[\sum_{k=1}^{\omega_i}\sum_{l=1}^{\omega_j}b_{ij,kl}g_{ij,kl}\right] - \sum_{i=1}^{m}\sum_{k=1}^{\omega_i-1}x_i[g_{ii,k,k+1}-1] \tag{4}$$

where m is the number of components and x_i is the mole fraction of component i. The number of effective hard spheres per molecule of component i is designated by ω_i. In a binary protein system, eqation (4) is redefined as follow :

$$\begin{aligned}\left(\frac{P}{\rho kT}\right)_{ref} &= 1+\rho\{x_1^2[\omega_{1A}^2 b_{AA}g_{AA}+2\omega_{1A}\omega_{1B}b_{AB}g_{AB}+\omega_{1B}^2 b_{BB}g_{BB}]\\ &+2x_1x_2[\omega_{1A}\omega_{2A}b_{AA}g_{AA}+\omega_{1A}\omega_{2B}b_{AB}g_{AB}+\omega_{1B}^2\omega_{2A}^2 b_{AB}g_{AB}\\ &+\omega_{1B}^2\omega_{2B}^2 b_{BB}g_{BB}]+x_2^2[\omega_{2A}^2 b_{AA}g_{AA}+2\omega_{2A}\omega_{2B}b_{AB}g_{AB}\\ &+\omega_{2B}^2 b_{BB}g_{BB}]\}-\{x_1(\omega_1-1)[X^2(g_{AA}-1)+2X(1-X)(g_{AB}-1)\\ &+(1-X)^2(g_{BB}-1)]+x^2(\omega_2-1)[Y^2(g_{AA}-1)\\ &+2Y(1-Y)(g_{AB}-1)+(1-Y)^2(g_{BB}-1)]\}\end{aligned} \tag{5}$$

where $\omega_{i\alpha}$ (i = 1,2 and $\alpha = A,B$) is the number of protein molecule α in component i per pre-aggregated protein particle: $\omega_{1A} = X\omega_A$, $\omega_{1B} = (1\text{-}X)\omega_B$, $\omega_{2A} = Y\omega_A$ and $\omega_{2B} = (1\text{-}Y)\omega_B$. $x_i = N_i/N$ is the fraction of i type pre-aggregated particle, g_{ij} is the $ij(i,j = A,B)$ pair radial distribution function of hard-sphere mixtures at contact, ω_i is the degree of pre-aggregation for component i and $b_{\alpha\beta}$ is the combined-second virial coefficient of hard sphere

$$b_{\alpha\beta} = \frac{2\pi\rho}{3}d_{\alpha\beta}^3 \tag{6}$$

where $d_{\alpha\beta}$ is the combined-effective hard sphere diameter

$$d_{\alpha\beta} = \frac{d_{\alpha\alpha}+d_{\beta\beta}}{2} \tag{7}$$

where $d_{\alpha\alpha}$ and $d_{\beta\beta}$ are the effective hard-sphere diameters for pure fluids α and β, respectively.

To obtain explicit equation of state from equation (4), a suitable mathematical form for $g_{\alpha\beta}(d^+_{\alpha\beta})$ is needed.[26]

$$g_{\alpha\beta}(\eta,\xi_{\alpha\beta}) = \frac{1}{1-\eta}+\frac{3}{2}\frac{\xi_{\alpha\beta}}{(1-\eta)^2}+\frac{1}{2}\frac{\xi_{\alpha\beta}^2}{(1-\eta)^3} \tag{8}$$

In protein mixtures, the packing fraction η is defined

$$\eta = \frac{\rho}{4}\{x_1(\omega_{1A}b_{AA}+\omega_{1B}b_{BB})+x_2(\omega_{2A}b_{AA}+\omega_{2B}b_{BB})\} \tag{9}$$

$$\xi_{\alpha\beta} = \left(\frac{b_{\alpha\alpha}b_{\beta\beta}}{b_{\alpha\beta}}\right)^{1/3}\frac{\rho}{4}\{x_1(\omega_{1A}b_{AA}+\omega_{1B}b_{BB}) + x_2(\omega_{2A}b_{AA}+\omega_{2B}b_{BB})\} \tag{10}$$

For one-component systems and equal-segment-size mixtures, $\xi_{\alpha\beta} = \eta$, and equation (4) reduces to the Carnahan-Starling equation for hard spheres.[30]

The perturbation term is

$$\left(\frac{P}{\rho kT}\right)_{pert} = \frac{\rho U^{total}}{2kT} \tag{11}$$

where U^{total}/kT is the total interaction energy of all pairs

$$\frac{U^{total}}{kT} = \sum_{i,j=1}^{m}x_i x_j\frac{U_{ij}}{kT} \tag{12}$$

where x_i is the mole fraction of the component i and U_{ij} is the total interaction energy for i-j pair (i,j = 1,2).

$$\frac{U_{11}}{kT} = \omega_{1A}^2\frac{U_{AA}}{kT}+\omega_{1A}\omega_{1B}\frac{U_{AB}}{kT}+\omega_{1B}^2\frac{U_{BB}}{kT} \tag{13}$$

$$\frac{U_{12}}{kT} = \omega_{1A}\omega_{2A}\frac{U_{AA}}{kT}+(\omega_{1A}\omega_{2B}+\omega_{2A}\omega_{1B})\frac{U_{AB}}{kT}+\omega_{1B}\omega_{2B}\frac{U_{BB}}{kT} \tag{14}$$

$$\frac{U_{22}}{kT} = \omega_{2A}^2\frac{U_{AA}}{kT}+\omega_{2A}\omega_{2B}\frac{U_{AB}}{kT}+\omega_{2B}^2\frac{U_{BB}}{kT} \tag{15}$$

where

$$\frac{U_{\alpha\beta}}{kT} = 4\pi\int_{d_{\alpha\beta}+2\Delta r}^{\infty}\left[\frac{W_{\alpha\beta}^{overall}(r)}{kT}r^2\right]dr,(\alpha,\beta=A,B) \tag{16}$$

where $W_{\alpha\beta}^{overall}(r)$ is the protein-protein perturbation potential of mean force for the α-β pair. The equation of state is given by

$$\begin{aligned}\frac{P}{\rho kT} &= \left(\frac{P}{\rho kT}\right)_{ref}+\left(\frac{P}{\rho kT}\right)_{pert}\\ &= 1+\rho\{x_1^2[\omega_{1A}^2 b_{AA}g_{AA}+2\omega_{1A}\omega_{1B}b_{AB}g_{AB}+\omega_{1B}^2 b_{BB}g_{BB}]\\ &+2x_1x_2[\omega_{1A}\omega_{2A}b_{AA}g_{AA}+\omega_{1A}\omega_{2B}b_{AB}g_{AB}+\\ &+\omega_{1B}^2\omega_{2A}^2 b_{AB}g_{AB}+\omega_{1B}^2\omega_{2A}^2 b_{BB}g_{BB}]\\ &+x_2^2[\omega_{2A}^2 b_{AA}g_{AA}+2\omega_{2A}\omega_{2B}b_{AB}g_{AB}+\omega_{2B}^2 b_{BB}g_{BB}]\}\\ &-\{x_1(\omega_1-1)[X^2(g_{AA}-1)+2X(1-X)(g_{AB}-1)\\ &+(1-X)^2(g_{BB}-1)]+x_2(\omega_2-1)[Y^2(g_{AA}-1)\\ &+2Y(1-Y)(g_{AB}-1)+(1-Y)^2(g_{BB}-1)]\}+\frac{\rho U^{total}}{2kT}\end{aligned} \tag{17}$$

The general equation for calculating the Helmholtz

energy is

$$\frac{A}{NkT} = \sum_i^m x_i \frac{A_i^o}{N_i kT} + \int_0^p \left(\frac{P}{\rho kT} - 1\right)\frac{d\rho}{\rho} + \sum_i^m x_i ln(x_i \rho kT) \quad (18)$$

Then, the chemical potential is

$$\Delta\mu_k = \left(\frac{\partial A}{\partial N_k}\right)_{T,V,N_{i\neq k}} \quad (19)$$

The derivations are shown in Appendix 1.

Solid Phase. For the solid phase, the reference equation of state is given by[31]:

$$\left(\frac{P}{kT}\right)_{ref} = \rho\left[\frac{3}{V^*-1} + 2.566 + 0.55(V^*-1) - 1.19(V^*-1)^2 + 5.59(V^*-1)^3\right] - 5.95V^{*3}/3 + 15.022 + \sum_{i=1}^{2} x_i ln(x_i) \quad (20)$$

where

$$V^* = V/V_0,\ V_0 = Nd_0^3/\sqrt{2} : d_0^3 = x_1^2 d_{AA}^3 + 2f(\alpha)x_1x_2d_{AB}^3 + x_2^2 d_{BB}^3.$$

Here, parameter α is the ratio of smaller to larger hard-sphere diameters. In this work, $d_{AA} \geq d_{BB}$ is used so that $\alpha = d_{BB}/d_{AA}$ and the function $f(\alpha)$ is determined by fitting to fit the computer-generated fluid-solid coexistence curves for binary hard-sphere mixtures in the range $0.85 \leq \alpha \leq 1$[31].

$$f(\alpha) = 1 + 13.5(1-\alpha)^{2.5} \quad (21)$$

Equations (20) and (21) are based on the fit to the computer generated compressibility factor for an one-component hard-sphere melting point. The perturbation of the solid phase is the same as that of the fluid phase, but the energy is represented by the difference of the number density.

The final form of equation, therefore, is

$$\left(\frac{P}{kT}\right) = \left(\frac{P}{kT}\right)_{ref} + \left(\frac{P}{kT}\right)_{pert} = \rho\left[\frac{3}{V^*-1} + 2.566 + 0.55(V^*-1) - 1.19(V^*-1)^2 + 5.59(V^*-1)^3\right] - 5.95V^{*3}/3 + 15.022 + \sum_i^m x_i ln(x_i) + \frac{\rho U^{total}}{2kT} \quad (22)$$

The Helmholtz energy and chemical potential of the solid phase are also derived from equaitons (18) and (19).

For aqueous solutions containing two kinds of proteins, the equilibrium condition is

$$\Delta\mu_1^{fluid} = \Delta\mu_1^{solid} \quad (23)$$

$$\Delta\mu_2^{fluid} = \Delta\mu_2^{solid} \quad (24)$$

$$P^{fluid} = P^{solid} \quad (25)$$

where subscripts "1" and "2" represent species of proteins. The derivations are shown in Appendix 1.

Results and Conclusion

Effect of Salt Concentration and Disparity of the Protein Size. Figures 2 and 3 represent the dependence of the salt concentration and the disparity of the protein size in the case of the non pre-aggregation ($\omega_{PA} = 1$).

Figure 2 shows the effect of the salt concentration for the systems with $H/kT = 8.9$, $\Delta r = 0.08$ nm, $\varepsilon/kT = 0.2$ nm, $\delta = 0.3$ nm, $d_s = 0.694$ nm, $d_{AA} = 3.5$ nm and $d_{BB} = 3.4$ nm. The solubility of globular proteins increases with the salt concentration. The composition difference between fluid and

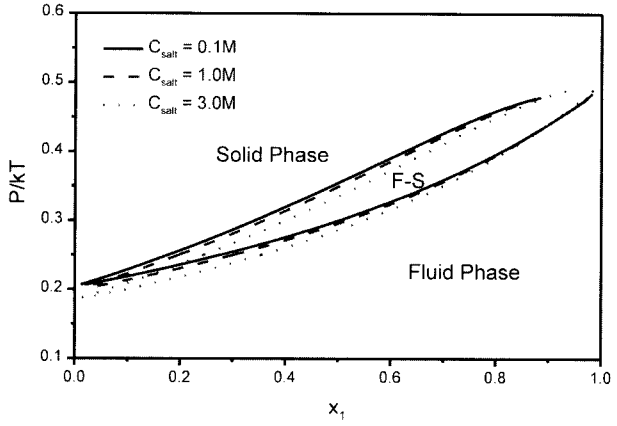

Figure 2. Theoretical phase diagrams for aqueous protein mixtures with different : C_{salt} : $H/kT = 8.9$, $\Delta r = 0.08$ nm, $\varepsilon/kT = 0.2$, $\delta = 0.3$ nm, $d_s = 0.694$ nm, $d_{11} = 3.5$ nm, $d_{22} = 3.4$ nm.

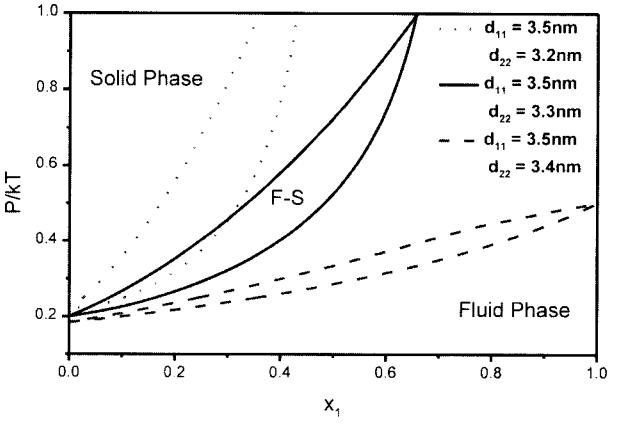

Figure 3. Theoretical phase diagrams for aqueous protein mixtures with different size d_{22} : $H/kT = 8.9$, $\Delta r = 0.08$ nm, $\varepsilon/kT = 0.2$, $\delta = 0.3$ nm, $d_s = 0.694$ nm, $C_{salt} = 3$ M.

solid phases at the lower salt concentration is slightly greater than that of the higher salt concenration.

Figure 3 shows the effect of the size difference between protein-A and protein-B. Their parameter values are H/kT = 8.9, Δr = 0.08 nm, ε/kT=0.2, δ=0.3 nm, d_s=0.694 nm, and C_{salt}=3 M for various d_{BB} and fixed d_{AA}=3.5 nm. The protein solubility decreases with increasing the size of protein-B. At fixed size of protein-A, the mean size of protein increases with the size of protein-B. It is correspondent with the size effect for the single protein system, that is, large solute molecules separate more effectively than small molecules.[32]

The composition difference between fluid and solid phases at a given composition of the fluid phase decreases with increasing the value of the disparity in protein size and salt concentration. Further, the protein size difference is more effective in the salt-induced protein precipitation than the increase of the salt concentration is.

Effect of Various Types of Pre-aggregation. Figures 4~8 represent phase diagrams of binary protein systems with various types of pre-aggregation.

Figure 4 shows the effect of the degree of homo-type pre-aggregation in component-1 only with H/kT= 8.9, Δr= 0.08 nm, ε/kT=0.2, δ=0.3 nm, d_s=0.694 nm, C_{salt}=3 M, d_{AA} =3.5 nm and d_{BB}=3.4 nm. Larger composition difference between fluid and solid phases at the given composition of the fluid phase is observed as the value of pre-aggregation for component-1 increases. It is correspondent with the result in Figure 3, the larger value of protein size disparity results in the less composition difference. It can be inferred that pre-aggregation of protein shows the similar effect to that of protein size.

Figure 5 shows phase diagrams calculated at X = 0.8, 0.9 and 1.0 in the case of random-type pre-aggregation in component-1 and non pre-aggregation in component-2 for the given system with ω_1 = 1.05, ω_2 = 1.00, H/kT= 8.9, Δr=0.08 nm, ε/kT=0.2, δ=0.3 nm, d_s=0.694 nm, C_{salt}=3 M, d_{AA} =3.5 nm and d_{BB}=3.4 nm. As the pre-aggregation fraction in component-1 decreases, fluid-solid coexistence region increases and the protein solubility decreases.

Figures 6~7 represent phase diagrams for the same degree of pre-aggregation in component-1 and 2 (ω_1 = 1.05, ω_2 = 1.05) at various pre-aggregation fraction of each protein in each component.

Figure 6 shows the binary protein system with H/kT=8.9, Δr=0.08 nm, ε/kT=0.2, δ=0.3 nm, d_s=0.694 nm, C_{salt}=3 M, d_{AA} =3.5 nm and d_{BB}=3.4 nm. The component-1 is set to have the alternate composition of component-2 (i.e., X is equal to 1-Y, and vice versa). It is apparent that the fluid-solid coexistence region becomes larger as fraction of both protein-B in component-1 and protein-A in component-2 increase. The size disparity between two components increases as X and 1-Y increase. This result is correspondent with that of Figure 4 ; larger size difference between two components leads to higher osmotic pressure and lower solubility.

Figure 7 shows phase diagram for the pre-aggregated pro-

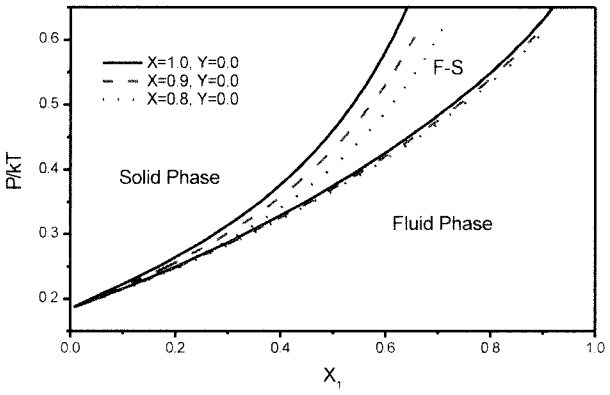

Figure 5. Theoretical phase diagrams for aqueous protein mixtures: C_{salt}=3.0 M, H/kT=8.9, Δr=0.08 nm, ε/kT=0.2, δ=0.3 nm, d_s=0.694 nm, d_{11}=3.5 nm, d_{22}=3.4 nm, ω_1=1.05, ω_2=1.0.

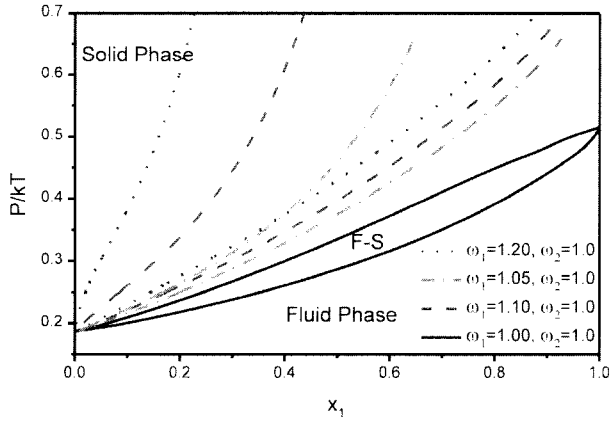

Figure 4. Theoretical phase diagrams for aqueous protein mixtures: C_{salt}=3.0 M, H/kT=8.9, Δr=0.08 nm, ε/kT=0.2, δ=0.3 nm, d_s=0.694 nm, d_{11}=3.5 nm, d_{22}=3.4 nm, X=1.0, Y=0.0.

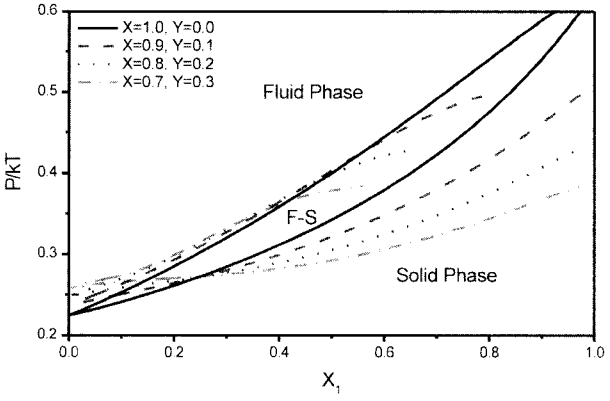

Figure 6. Theoretical phase diagrams for aqueous protein mixtures: C_{salt}=3.0 M, H/kT=8.9, Δr=0.08 nm, ε/kT=0.2, δ=0.3 nm, d_s=0.694 nm, d_{11}=3.5 nm, d_{22}=3.4 nm, ω_1=1.05, ω_2=1.05.

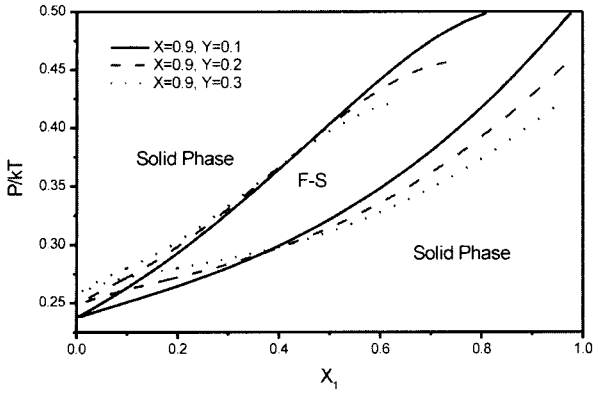

Figure 7. Theoretical phase diagrams for aqueous protein mixtures: $C_{salt}=3.0$ M, $H/kT=8.9$, $\Delta r=0.08$ nm, $\varepsilon/kT=0.2$, $\delta=0.3$ nm, $d_s=0.694$ nm, $d_{11}=3.5$ nm, $d_{22}=3.4$ nm, $\omega_1=1.05$, $\omega_2=1.05$.

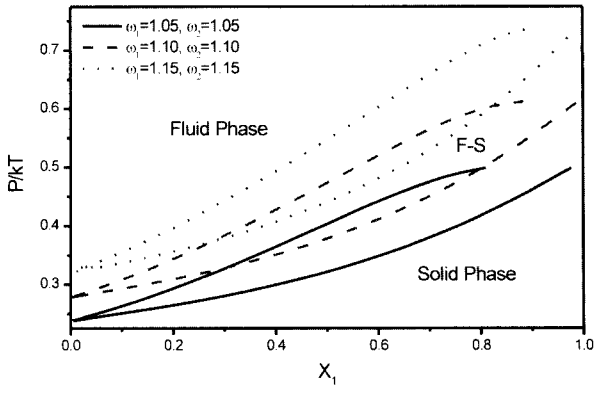

Figure 8. Theoretical phase diagrams for aqueous protein mixtures: $C_{salt}=3.0$ M, $H/kT=8.9$, $\Delta r=0.08$ nm, $\varepsilon/kT=0.2$, $\delta=0.3$ nm, $d_s=0.694$ nm, $d_{11}=3.5$ nm, $d_{22}=3.4$ nm, $X=0.9$, $Y=0.1$.

tein mixture at various fraction of protein-A in component-2 at $X=0.9$, $\omega_1=1.05$, and $\omega_2=1.05$, with $H/kT=8.9$, $\Delta r=0.08$ nm, $\varepsilon/kT=0.2$, $\delta=0.3$ nm, $d_s=0.694$ nm, $C_{salt}=3$ M, $d_{AA}=3.5$ nm and $d_{BB}=3.4$ nm, In such a case, the increase of Y, which means the content of protein-A in component-2, minimizes the size difference between two components. As Y increases with fixed value for X, the osmotic pressure increases in component-1-poor regions and decreases in component-1-rich regions, respectively. Increase of osmotic pressure in component-1-poor region is due to the size increase in component-2. As the composition for the component-1 increase, the osmotic pressure increases due to the effect for size disparity.

Figure 8 shows a phase diagram for the systems of binary protein mixtures for $X=0.9$ and $Y=0.1$, with $H/kT=8.9$, $\Delta r=0.08$ nm, $\varepsilon/kT=0.2$, $\delta=0.3$ nm, $d_s=0.694$ nm, $C_{salt}=3$ M, $d_{AA}=3.5$ nm and $d_{BB}=3.4$ nm, varying with degrees of pre-aggregation ($\omega_1=\omega_2=1.05$, $\omega_1=\omega_2=1.10$ and $\omega_1=\omega_2=1.15$). As shown in this figure, phase diagram is shifted to higher osmotic pressure the degree of pre-aggregation increase. It means that the size growth of each component diminishes the solubility of protein. Single protein systems[32] also show the similar result that the pre-aggregation leads to the poor solubility of protein.

Results show that the pre-aggregation in the binary protein systems strongly influences on the proteins precipitation. The increment of the degree of pre-aggregation is proved to have the similar effect to that of the size increase of protein particles, which is the decrease of the solubility of protein. Furthermore, the phase behaviors of binary protein systems depend on the various types of pre-aggregation.

It is amazing that the small change of the degree of pre-aggregation, ω affects to the phase behavior of protein mixture. It means that since the small irreversible aggregation of protein gives the effect to enlarge the protein size, the interaction between protein molecules gets more attractive. However, it is well known that protein surface chemistry plays a very important role in phase behavior of protein mixture solutions; nevertheless, our model does not give the information on protein surface condition. Such as charge distribution, hydrophobic or hydrophilic surface fraction. Unfortunately, there are not experimental data in any open literature; therefore, we cannot compare our model with them.

Consequently, Our model applies the equation of state for random copolymer blends to the pre-aggregated protein mixture. According to the previous[36] and present results, ω does not exceed 2.0, which means the sequence of protein particles is not significant and protein molecules aggregate not totally but partially. That point makes it reasonable to apply the model to the binary protein aggregation systems.

Appendix 1

Fluid Phase. The Helmholtz Energy of the fluid phase is derived by equation (18),

$$\frac{A}{NkT}=\left[\frac{A}{NkT}\right]_{ref}+\left[\frac{A}{NkT}\right]_{pert}$$

$$=\sum_{i=1}^{2}\left[\frac{A_i^0}{NkT}\right]_{ref}+\rho\{x_1^2[\omega_{1A}^2 b_{AA}W_{AA}+2\omega_{1A}\omega_{1B}b_{AB}W_{AB}$$

$$+\omega_{1B}^2 b_{BB}W_{BB}]+2x_1x_2[\omega_{1A}\omega_{2A}b_{AA}W_{AA}+\omega_{1A}\omega_{2B}b_{AB}W_{AB}$$

$$+\omega_{1B}\omega_{2A}b_{AB}W_{AB}+\omega_{1B}\omega_{2B}b_{BB}W_{BB}]$$

$$+x_2^2[\omega_{2A}^2 b_{AA}W_{AA}+2\omega_{2A}\omega_{2B}b_{AB}W_{AB}+\omega_{2B}^2 b_{BB}W_{BB}]$$

$$-\{x_1(\omega_1-1)[X^2Q_{AA}+2X(1-X)Q_{AB}+(1-X)^2Q_{BB}]$$

$$+x_2(\omega_2-1)[Y^2Q_{AA}+2Y(1-Y)Q_{AB}+(1-Y)^2Q_{BB}]\}$$

$$+\{x_1 ln(x_1\rho kT)+x_2 ln(x_2\rho kT)\}+\frac{\rho U^{total}}{2\ kT} \qquad \text{(A1)}$$

where

$$W_{\alpha\beta}=\frac{I_1}{\eta}+\frac{3}{2}\frac{\xi_{\alpha\beta}}{\eta}I_2+\frac{1}{2}\frac{\xi_{\alpha\beta}^2}{\eta}I_3 \tag{A2}$$

$$Q_{\alpha\beta}=\frac{I_1}{\eta}+\frac{3}{2}\frac{\xi_{\alpha\beta}}{\eta^2}I_2+\frac{1}{2}\frac{\xi_{\alpha\beta}^2}{\eta^3}I_3 \tag{A3}$$

$$I_1=-ln(1-\eta),\quad I_n=-I_{n-1}+\frac{1}{1-\eta}\frac{\eta^{n-1}}{(1-\eta)^{n-1}} \tag{A4}$$

The chemical potential of the fluid phase is given by

$$\begin{aligned}\frac{\Delta\mu_k}{kT}&=\left[\frac{\Delta\mu_k}{kT}\right]_{ref}+\left[\frac{\Delta\mu_k}{kT}\right]_{pert}\\
&=2\rho\{x_1^2\omega_1^2[X^2b_{AA}W_{AA}+2X(1-X)b_{AB}W_{AB}\\
&+(1-X)^2b_{BB}W_{BB}]+2x_1x_2\omega_1\omega_2[XYb_{AA}W_{AA}\\
&+X(1-Y)b_{AB}W_{AB}+(1-X)Yb_{AB}W_{AB}\\
&+(1-X)(1-X)b_{BB}W_{BB}]+x_2^2\omega_2^2[Y^2b_{AA}W_{AA}\\
&+2Y(1-Y)b_{AB}W_{AB}+(1-Y)^2b_{BB}W_{BB}]\}\\
&-\{x_1(\omega_1-1)[X^2Q_{AA}+2X(1-X)Q_{AB}+(1-X)^2Q_{BB}]\\
&+x_2(\omega_2-1)[Y^2Q_{AA}+2Y(1-Y)Q_{AB}+(1-Y)^2Q_{BB}]\}\\
&+\rho\left\{2x_1\left[N\frac{\partial x_1}{\partial N_k}\right]\omega_1^2[X^2b_{AA}W_{AA}+2X(1-X)b_{AB}W_{AB}\right.\\
&+(1-X)^2b_{BB}W_{BB}]+2\left[N\frac{\partial x_1}{\partial N_k}\right]x_2\omega_1\omega_2[XYb_{AA}W_{AA}\\
&+X(1-Y)b_{AB}W_{AB}+(1-X)Yb_{AB}W_{AB}+(1-X)(1-Y)b_{BB}W_{BB}]\\
&+2x_1\left[N\frac{\partial x_2}{\partial N_k}\right]\omega_1\omega_2[XYb_{AA}W_{AA}+X(1-Y)b_{AB}W_{AB}\\
&+(1-X)Yb_{AB}W_{AB}+(1-X)(1-Y)b_{BB}W_{BB}]\\
&+2x_2\left[N\frac{\partial x_2}{\partial N_k}\right]\omega_2^2[Y^2b_{AA}W_{AA}+2Y(1-Y)b_{AB}W_{AB}\\
&+(1-Y)^2b_{BB}W_{BB}]\}-\left\{\left[N\frac{\partial x_1}{\partial N_k}\right](\omega_1-1)[X^2Q_{AA}\right.\\
&+2X(1-X)Q_{AB}+(1-X)^2Q_{BB}+\left[N\frac{\partial x_2}{\partial N_k}\right](\omega_2-1)[Y^2Q_{AA}\\
&+2Y(1-Y)Q_{AB}+(1-Y)^2Q_{BB}]\}\\
&+\rho\left\{x_1^2\omega_1^2\left\langle X^2b_{AA}\left[N\frac{\partial W_{AA}}{\partial N_k}\right]+2X(1-X)b_{AB}\left[N\frac{\partial W_{AB}}{\partial N_k}\right]\right.\right.\\
&+(1-X)^2b_{BB}\left[N\frac{\partial W_{BB}}{\partial N_k}\right]\rangle+2x_1x_2\omega_1\omega_2\left\langle XYb_{AA}\left[N\frac{\partial W_{AA}}{\partial N_1}\right]\right.\\
&+X(1-Y)b_{AB}\left[N\frac{\partial W_{AB}}{\partial N_1}\right]+(1-X)Yb_{AB}\left[N\frac{\partial W_{AB}}{\partial N_1}\right]\\
&+(1-X)(1-Y)b_{BB}\left[N\frac{\partial W_{BB}}{\partial N_1}\right]\rangle\\
&+x_2^2\omega_2^2\left\langle Y^2b_{AA}\left[N\frac{\partial W_{AA}}{\partial N_k}\right]+2Y(1-Y)b_{AB}\left[N\frac{\partial W_{AB}}{\partial N_k}\right]\right.\\
&\left.\left.+(1-Y)^2b_{BB}\left[N\frac{\partial W_{BB}}{\partial N_k}\right]\rangle\right\}-\left\{x_1(\omega_1-1)\left\langle X^2\left[N\frac{\partial Q_{AA}}{\partial N_k}\right]\right.\right.\\
&+2X(1-X)\left[N\frac{\partial Q_{AB}}{\partial N_k}\right]+(1-X)^2\left[N\frac{\partial Q_{BB}}{\partial N_k}\right]\rangle\\
&+x_2(\omega_2-1)\left\langle Y^2\left[N\frac{\partial Q_{AA}}{\partial N_k}\right]+2Y(1-Y)\left[N\frac{\partial Q_{AB}}{\partial N_k}\right]\right.\\
&\left.\left.+(1-Y)^2\left[N\frac{\partial Q_{BB}}{\partial N_k}\right]\rangle\right\}+ln(x_k\rho kT)+1+\rho\frac{U^{total}}{kT}\\
&+\frac{\rho}{2}\left[N\frac{\partial(U^{total}/kT)}{\partial N_k}\right]\end{aligned} \tag{A5}$$

where

$$\begin{aligned}\left[N\frac{\partial(U^{total}/kT)}{\partial N_k}\right]&=4\pi\left\{2x_1\left[N\frac{\partial x_1}{\partial N_k}\right]\frac{U_{11}}{kT}+2x_2\left[N\frac{\partial x_1}{\partial N_k}\right]\frac{U_{12}}{kT}\right.\\
&\left.+2x_1\left[N\frac{\partial x_2}{\partial N_k}\right]\frac{U_{12}}{kT}+2x_2\left[N\frac{\partial x_2}{\partial N_k}\right]\frac{U_{22}}{kT}\right\}\end{aligned} \tag{A6}$$

$$\left(N\frac{\partial W_{\alpha\beta}}{\partial N_k}\right)=\left(\frac{\partial W_{\alpha\beta}}{\partial\eta}\right)\left(N\frac{\partial\eta}{\partial N_k}\right)+\left(\frac{\partial W_{\alpha\beta}}{\partial\xi_{\alpha\beta}}\right)\left(N\frac{\partial\xi_{\alpha\beta}}{\partial N_k}\right) \tag{A7}$$

$$\left(N\frac{\partial Q_{\alpha\beta}}{\partial N_k}\right)=\left(\frac{\partial Q_{\alpha\beta}}{\partial\eta}\right)\left(N\frac{\partial\eta}{\partial N_k}\right)+\left(\frac{\partial Q_{\alpha\beta}}{\partial\xi_{\alpha\beta}}\right)\left(N\frac{\partial\xi_{\alpha\beta}}{\partial N_k}\right) \tag{A8}$$

$$\left[\frac{\partial W_{\alpha\beta}}{\partial\eta}\right]=-\frac{I_1}{\eta^2}+\frac{1}{\eta}\left[\frac{\partial I_1}{\partial\eta}\right]-3\frac{\xi_{\alpha\beta}}{\eta^3}I_2+\frac{3}{2}\frac{\xi_{\alpha\beta}}{\eta^2}\left[\frac{\partial I_2}{\partial\eta}\right]-\frac{3}{2}\frac{\xi_{\alpha\beta}^2}{\eta^3}\left[\frac{\partial I_3}{\partial\eta}\right] \tag{A9}$$

$$\left[\frac{\partial I_1}{\partial\eta}\right]=\frac{1}{1-\eta} \tag{A10}$$

$$\left[\frac{\partial I_2}{\partial\eta}\right]=-\left[\frac{\partial I_1}{\partial\eta}\right]+\frac{1}{(1-\eta)^2} \tag{A11}$$

$$\left[\frac{\partial I_3}{\partial\eta}\right]=-\left[\frac{\partial I_2}{\partial\eta}\right]+\frac{\eta}{(1-\eta)^3} \tag{A12}$$

$$\left[\frac{\partial W_{\alpha\beta}}{\partial\xi_{\alpha\beta}}\right]=\frac{3}{2}\frac{I_2}{\eta^2}+\frac{\xi_{\alpha\beta}}{\eta^3}I_3 \tag{A13}$$

$$\left[\frac{\partial Q_{\alpha\beta}}{\partial\eta}\right]=\frac{1}{1-\eta}-\frac{3}{2}\frac{\xi_{\alpha\beta}}{(1-\eta)^2}-\frac{1}{2}\frac{\xi_{\alpha\beta}^2}{(1-\eta)^3} \tag{A14}$$

$$\left[\frac{\partial Q_{\alpha\beta}}{\partial\xi_{\alpha\beta}}\right]=\frac{3}{2}\frac{1}{1-\eta}+\frac{1}{2}\frac{\xi_{\alpha\beta}}{(1-\eta)^2} \tag{A15}$$

Solid Phase.

The helmholtz energy is

$$\frac{A}{NkT}=\left(\frac{A}{NkT}\right)_{ref}+\left(\frac{A}{NkT}\right)_{pert}$$
$$-3ln\left(\frac{V^*-1}{V^*}\right)+5.124ln(V^*)-20.78V^*+9.52V^{*2} \quad \text{(A16)}$$
$$-5.95V^{*3}/3+15.022+\sum_{i=1}^{2}x_i lnx_i+\frac{\rho U^{total}}{2\ kT}$$

The chemical potential is

$$\left(\frac{\Delta\mu_k}{kT}\right)=\left(\frac{\Delta\mu_k}{kT}\right)_{ref}+\left(\frac{\Delta\mu_k}{kT}\right)_{pert}$$
$$=\left(\frac{A}{NkT}\right)_{ref}+\left[3\frac{1}{V^*(1-V^*)}+5.124\frac{1}{V^*}-5.95V^{*2}\right. \quad \text{(A17)}$$
$$\left.+19.04V^*-20.78\right]\times\left(N\frac{\partial V^*}{\partial N_k}\right)+15.022+ln(x_k)$$
$$+\rho\frac{U^{total}}{kT}+\frac{\rho}{2}\left[N\frac{\partial(U^{total}/kT)}{\partial N_k}\right]$$

where

$$\left(N\frac{\partial V^*}{\partial N_k}\right)=\left(\frac{\partial V^*}{\partial\rho}\right)\left(N\frac{\partial\rho}{\partial N_k}\right)+\left(\frac{\partial V^*}{\partial d_o^3}\right)\left(N\frac{\partial d_o^3}{\partial N_k}\right) \quad \text{(A18)}$$

$$\left(\frac{\partial V^*}{\partial\rho}\right)=-\frac{\sqrt{2}}{\rho^2 d_o^3} \quad \text{(A19)}$$

$$\left(\frac{\partial V^*}{\partial d_o^3}\right)=-\frac{\sqrt{2}}{\rho(d_o^3)^2} \quad \text{(A20)}$$

$$\left(N\frac{\partial\rho}{\partial N_k}\right)=\rho \quad \text{(A21)}$$

$$\left(N\frac{\partial d_o^3}{\partial N_k}\right)=2\left\{x_1\left(N\frac{\partial x_1}{\partial N_k}\right)d_{AA}^3+f(\alpha)d_{AB}^3\left[\left(N\frac{\partial x_1}{\partial N_k}\right)x_2\right.\right. \quad \text{(A22)}$$
$$\left.\left.+x_1\left(N\frac{\partial x_2}{\partial N_k}\right)\right]+x_2\left(N\frac{\partial x_1}{\partial N_k}\right)d_{BB}^3\right\}$$

Appendix 2

Contributions to the effective two-body potentials for proteins in aqueous electrolyte solution.

1. The electric double-layer repulsion[10]:

$$\frac{W_{ij}^{elec}(r)}{kT}=\frac{z_i z_j e^2}{4\pi\varepsilon_o\varepsilon_r kT}\frac{e^{[-\kappa(r-d_p)]}}{r\left(1+\frac{\kappa d_{ii}}{2}\right)\left(1+\frac{\kappa d_{jj}}{2}\right)} \quad \text{(A23)}$$
$$\text{for} \quad r>(d_{ij}+2\Delta r)$$

k : Boltzmann constant
T : absolute temperature
z_i : valence of the species i
e : the unit of electron charge
d_{ii} : the diameter of species i
$d_{ij}=(d_{ii}+d_{ij})/2$
$4\pi\varepsilon_0$: the dielectric permittivity of free space
ε_r : the relative dielectric permittivity of water
Δr : the effective-sphere hydration/stern layer
κ : the inverse of the Debye length; given by $\kappa^2=(2e^2N_AI)/(kT\varepsilon_0\varepsilon)$
N_A : Avogadro's number
I : the ionic strength of the salt, given by $I=(z_{an}^2\rho_{an}+z_{cat}^2\rho_{cat})/2$
z_{an} and z_{cat}: the anion and cation valences, respectively
ρ_{an} and ρ_{cat}: the ionic number densities.

2. The attractive Hamaker dispersion interaction[10,33]:

$$\frac{W_{ij}^{disp}(r)}{kT}=-\frac{H}{6}\left[\frac{d_{ii}d_{jj}}{r^2-d_{ij}^2}+\frac{d_{ii}d_{jj}}{r^2-\frac{(d_{ii}-d_{jj})^2}{4}}+2ln\left[\frac{r^2-d_{ij}^2}{r^2-\frac{(d_{ii}-d_{jj})^2}{4}}\right]\right]$$
$$\text{for} \quad r>d_p+2\Delta r \quad \text{(A24)}$$

H: the effective Hamaker constant for the protein-protein interaction

3. The osmotic attractive interaction potential[19]:

$$\frac{W_{ij}^{osmotic}(r)}{kT}=-\frac{2\pi\rho_s}{3}\left[\left(\frac{d_{iis}}{2}\right)^3+\left(\frac{d_{jjs}}{2}\right)^3\right]$$
$$\times\left[1+\frac{r^3}{8\left[\left(\frac{d_{iis}}{2}\right)^3+\left(\frac{d_{jjs}}{2}\right)^3\right]}-\frac{3}{4}\frac{r\left[\left(\frac{d_{iis}}{2}\right)^2+\left(\frac{d_{jjs}}{2}\right)^2\right]}{\left[\left(\frac{d_{iis}}{2}\right)^3+\left(\frac{d_{jjs}}{2}\right)^3\right]}\right. \quad \text{(A25)}$$
$$\left.-\frac{3}{8r}\frac{\left[\left(\frac{d_{iis}}{2}\right)^2+\left(\frac{d_{jjs}}{2}\right)^2\right]^2}{\left[\left(\frac{d_{iis}}{2}\right)^3+\left(\frac{d_{jjs}}{2}\right)^3\right]}\right]$$
$$for \quad d_{ij}<r<d_{ijs}+2\Delta r$$

ρ_s : the total ionic number density

$d_{iis}=(d_{ii}+d_s)/2$

$d_s=(z_{an}d_{cat}+z_{cat}d_{an})/(z_{cat}+z_{an})$: a valence-weighted ion diameter

4. The specific interaction[23,34]:

$$\frac{W_{specific}(s)}{kT}=-\frac{\varepsilon_{sp}}{kT} \quad for \quad d_p<r<(d_p+\delta) \quad \text{(A26)}$$

ε_{sp} and δ: model parameters

References

(1) P. R. Foster, P. Dunhill, and M. D. Lilly, *Biochem. Biophys. Acta*, **317**, 505 (1975).
(2) R. N. Haire, W. A. Tisel, J. C. White, and A. Rosenberg, *Biopolymers*, **23**, 2761 (1984).
(3) Y. C. Shih, H. W. Blanch, and J. M. Prausnitz, *Biotech. Bioeng.*, **40**, 1155 (1992).
(4) M. Q. Niederauer and C. E. Glatz, *Adv. Biochem. Eng. Technol.*, **47**, 159 (1992).
(5) F. Rothstein, *Protein Precipitation Process Engineering*, R. G. Harrion, Ed., Dekker, New York, 1994.
(6) P. A. Belter, E. L. Cussler, and W. S. Hu, *Bioseparations: Downstream Processing Operations*, Wiley, New York, 1998.
(7) F. Rothstein, *Protein Purification Process Engineering*, R. G. Harvision, Ed., Macel Dekker, New York, 1994.
(8) C. J. Coen, H. W. Blanch, and J. M. Prausnitz, *AIChE J.*, **41**, 1 (1995).
(9) J. Wu and J. M. Prausnitz, *Fluid Phase Equilibria*, **155**, 139 (1999).
(10) E. Verwey and J. Overbeek, *Theory of Stability of Lyophobic Colloids*, Elsevier, Amsterdam, 1948.
(11) S. Askura and F. Oosawa, *J. Polym. Sci.*, **33**, 183 (1958).
(12) A. Vrij, *Pure Appl. Chem.*, **48**, 471 (1976).
(13) J. F. Joanny, L. Leibler, and P. G. de Gennes, *J. Polym. Sci., Polym. Phys.*, **17**, 1073 (1979).
(14) H. De Hek and A. Vrij, *J. Colloid Interf. Sci.*, **41**, 996 (1995).
(15) A. P. Gast, C. K. Hall, and W. G. Russel, *J. Farad. Discuss. Chem. Soc.*, **76**, 189 (1983b).
(16) M. J. Grimson, *J. Chem. Soc. Farad. Trans.*, **79**, 817 (1983).
(17) J. M. Victor and J. P. Hansen, *J. Phys. Lett.*, **45**, L-307 (1984).
(18) H. Mahadevan and C. K. Hall, *AIChE J.*, **36**, 1517 (1990).
(19) H. Mahadevan and C. K. Hall, *AIChE J.*, **38**, 573 (1992).
(20) V. Vlachy and J. M. Prausnitz, *J. Phys. Chem.*, **96**, 6465 (1992).
(21) V. Vlachy, H. W. Blanch, and J. M. Prausnitz, *AIChE J.*, **39**, 215 (1993).
(22) Y. C. Chiew, *Molec. Phys.*, **70**, 129 (1990).
(23) D. Kuehner, H. W. Blanch, and J. M. Prausnitz, *Fluid Phase Equilibria*, **116**, 140 (1996).
(24) S. G. Kim and Y. C. Bae, *Korean J. Chem. Eng.*, **17**, 638 (2000).
(25) Y. Song, S. M. Lambert, and J. M. Prausnitz, *Macromolecules*, **27**, 441 (1994).
(26) Y. Song, S. M. Lambert, and J. M. Prausnitz, *Ind. Eng. Chem. Res.*, **33** 1047 (1994).
(27) Y. Song, S. M. Lambert, and J. M. Prausnitz, *Chem. Eng. Sci.*, **49**, 2765 (1994).
(28) T. Hino, Y. Song, and J. M. Prausnitz, *Macromolecules*, **27**, 5681 (1994).
(29) T. Hino, Y. Song, and J. M. Prausnitz, *J. Polym. Sci.*, **34**, 1977 (1996).
(30) N. F. Carnahan and K. E. Starling, *J. Chem. Phys.*, **51**, 635 (1969).
(31) D. A.Young, *J. Chem. Phys.*, **98**, 9819 (1993).
(32) P. A. Albertsson, *Partition of Cell Particles and Macromolecules*, Wiley, New York, 1986.
(33) H. C. Hamaker, *Physica IV*, **10**, 1058 (1937).
(34) D. Kuehner, C. Heyer, C. Ramsch, U. M. Fornefeld, H. W. Blanch, and J. M. Prausnitz, *Biophys. J.*, **73**, 3211 (1997).
(35) R. A. Curtis, C. Steinbrecher, M. Heinemann, H. W. Blanch, and J. M. Prausnitz, *Biophys. Chem.*, **98**, 249 (2002).
(36) S. G. Kim and Y. C. Bae, *Macromol. Res.*, **11**, 53 (2003).